Broadband Terahertz Isolator

Alexander N. Grebenchukov, Valentina I. Ivanova, Anton V. Suslov, Grigory I. Kropotov, and Mikhail K. Khodzitsky, *Member, IEEE,*

***Abstract*—Breaking reciprocity in optical systems is enabling the possibility of implementing devices with unidirectional wave propagation. Currently, there is an active search for suitable material with an efficient nonreciprocal response at the terahertz (THz) frequency range. Ideally, such material should allow low-loss operation without an external magnetic field at room temperature. Gyrotropic hexaferrite ceramic is highly promising for achieving optical isolation in the THz spectral range. Here, we demonstrate a broadband self-biased THz isolator based on magnetized aluminum-substituted barium hexaferrite. We reveal the necessary surface density of the hexaferrite sample for the realization of THz isolation. The proposed device exhibits no less than 30 dB of isolation from 0.2 to 1 THz. Moreover, we show that the gyrotropy properties of hexaferrite ceramics can be reasonably predicted by their magnetic properties. This device is expected to be useful for applications where one-way propagation of broadband THz wave is desired.**

***Index Terms*—Terahertz isolator, Nonreciprocal device, Faraday effect, M-type hexaferrite.**

I. Introduction

TERAHERTZ (THz) electromagnetic radiation is endowed with rich scientific and technological opportunities [1], [2], [3], applicable in a wide variety of fields, from spectroscopy [4] and sensing [5] to imaging [6] and communications [7]. However, recent development in intense THz sources and high-sensitive THz detectors make apparent the lack of efficient optical components operating in that frequency range, particularly nonreciprocal ones. Breaking Lorentz reciprocity results in new functionality that are unattainable for reciprocal systems [8], [9]. An isolator is a basic nonreciprocal device allowing to realize one-way radiation transmission. Such functionality allows canceling back reflections, which results in electromagnetic sources protection, noise reduction, impedance matching, and decoupling [10].

The main criteria for a high-performance isolator are broadband and high isolation, low insertion losses for propagation in a forward direction, and operation at room temperature without external magnetic field bias. Implementation of a THz isolator meeting all of these criteria is a challenging task. Several approaches have been applied for developing THz isolator, each of which has its own limitations and drawbacks. The utilization of space-time modulated media requires high-speed modulation of material parameters in time by external forces [11], [12], which is difficult in practical realization. Another mechanism is based on incorporating nonlinear materials [13]. In that case, isolation performance is fundamentally power-dependent and suffers from dynamic nonreciprocity constraints [14]. The most common way for isolator realization is based on magneto-optical (MO) effects. The operational principle of a typical MO isolator relies on 45° Faraday rotator and a pair of specifically oriented polarizers. After a round trip through such a system, the radiation acquires 90° polarization rotation in total and is blocked by the front polarizer. However, there is a lack of suitable THz MO materials for the realization of a high-performance THz isolator. Yttrium iron garnet (YIG) metasurface [15], two-dimensional materials [16], and high-mobility semiconductors, such as InSb [17] and HgTe [18] allow achieving giant Faraday rotation in the THz frequency range. Several THz isolators have been proposed based on InSb magnetoplasmonic properties [19], [20], [21], [22], [23]. In [24], the THz isolator based on a three-layer graphene stack has been demonstrated. However, all the proposed solutions are requiring an external magnetic field, which makes such isolators more complex and bulky. Another material enabling to realize complete THz isolator without applying external magnetic bias is magnetized ferrites [25], [26], which are distinguished by broadband Faraday rotation. Unfortunately, the performance of ferrite isolators is often limited by large insertion losses.

Within this context, it is highly desirable to find a new material enabling realization THz isolator operating without external bias at room temperature with superior magneto-optical properties over existing options. Trying to comply with these demands, recently, several studies were devoted to the characterization of hexaferrite ceramics in the THz frequency range [27], [28], [29], [30]. These works are focused on the investigation of commercially available hexaferrites. In [31], we have synthesized a new perspective hexaferrite ceramics (high-dense $BaAl_{1.4}Fe_{10.6}O_{19}$) for utilization as a Faraday rotator in the THz isolator.

In this paper, we fabricated the $BaAl_{1.4}Fe_{10.6}O_{19}$ hexaferrite samples of different thicknesses and densities. The Faraday rotation spectra of these longitudinally magnetized samples were measured in the THz frequency range at room temperature. The results show that Faraday rotation angle linearly depends on surface density of the samples. As a result, we revealed the suitable sample parameters for obtaining the required 45° rotation. Then, we assembled a THz isolator by placing a hexaferrite 45° Faraday rotator between a pair of polarizers and measured its isolation performance. Obtained isolation spectra exhibits broadband character. Moreover, we discuss the possibility to predict induced THz Faraday rotation utilizing only the magnetic characteristics of hexaferrites.

Manuscript received Month Date, 20xx; revised Month Date, 20xx. *(Corresponding author: Alexander Grebenchukov).*

A. N. Grebenchukov, G. I. Kropotov, and M. K. Khodzitsky are with Tydex LLC, 194292 St. Petersburg, Russia (e-mail: grebenchukovaleksandr@tydex.ru; grigorykropotov@tydex.ru; mikhailkhodzitskiy@tydex.ru).

V. I. Ivanova is with Ferrite-Domen Scientific Research Institute, St. Petersburg 196084, Russia (e-mail: ivanova_domen@mail.ru).

A. V. Suslov is with Herzen State Pedagogical University of Russia, St. Petersburg, 191186 Russia (e-mail: avsuslov@herzen.spb.ru).

II. Samples and Methods

The investigated $BaAl_{1.4}Fe_{10.6}O_{19}$ samples have been synthesized using iron (Fe_2O_3) and aluminum (Al_2O_3) oxides and barium carbonate ($BaCO_3$) with stoichiometric proportions in accordance with [31]. The components were mixed and annealed in air. Then, the resulting ferrite powder was pressed in a constant magnetic field of 795 kA/m. After pressing process, the samples were again annealed in an oxygen atmosphere. A total of 11 samples with different densities (ρ) and thicknesses (d) were fabricated. The thickness of the sample with $\rho = 4.91$ g/cm^3 was successively grounded off from 3.55 mm to 2.8 mm. The parameters of all investigated samples are listed in Table I.

TABLE I
Densities and thicknesses of $BaAl_{1.4}Fe_{10.6}O_{19}$ hexaferrite samples.

Sample №	Density, ρ (g/cm^3)	Thickness, d (mm)
1	5.068	1.0
2	5.129	1.17
3	5.061	1.3
4	5.081	1.43
5	4.95	2.0
6	5.076	2.38
7	4.91	2.8
8	4.91	2.9
9	4.91	3.0
10	4.91	3.25
11	4.91	3.55

The crystal structure of the samples was characterized at room temperature using diffractometer DRON-7 with Cu-K_α radiation source ($\lambda = 1.5406$ Å) in the 2θ range from 10° to 80°. Obtained X-ray diffraction (XRD) patterns were analyzed by the Rietveld method using the FullProf software [32]. The XRD pattern for a 2.8 mm-thick sample is presented in Fig. 1.

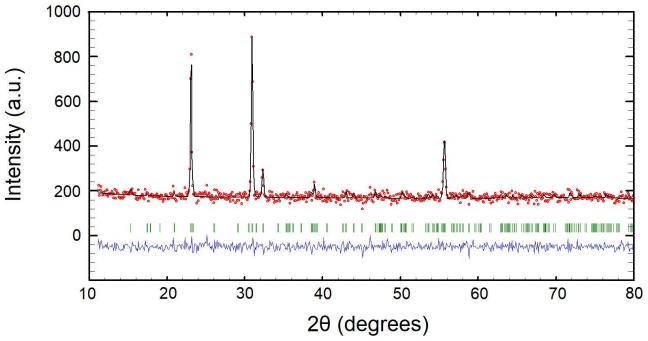

Fig. 1. X-ray diffraction pattern of $BaAl_{1.4}Fe_{10.6}O_{19}$. Red dots represent experimental data, a dark curve is calculated pattern by Rietveld method, green vertical bars are for the diffraction peaks position, and the lower blue curve is a difference between experimental and calculated data.

The studied sample has a hexagonal structure with space group $P6_3/mmc$. Extracted by Rietveld method lattice parameters $a = 5.867$ Å and $c = 23.119$ Å are well consistent with previously obtained values for aluminum-substituted barium hexaferrites [33].

The Faraday rotation spectra of hexaferrite samples were measured using the THz time-domain spectroscopy system (Menlo Systems TERA K8). A schematic representation of the experimental setup is shown in Fig. 2.

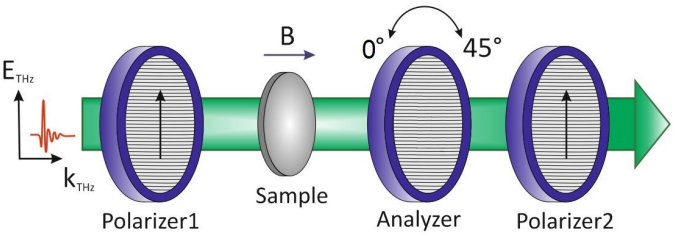

Fig. 2. Experimental THz polarimetry scheme.

To measure the Faraday rotation effect, the hexaferrite samples were preliminarily magnetized up to saturation. For the sample magnetization the static magnetic field of 795-955 kA/m was applied. The measurement scheme consists of two polarizers defining linear polarization for generated and detected signals. The magnetized $BaAl_{1.4}Fe_{10.6}O_{19}$ sample was placed between the first polarizer (set at 0°) and the analyzer. A rotatable linear polarizer was used as an analyzer. To evaluate the Faraday rotation, two measurements were performed for each sample when the analyzer was set at 0° and 45° positions, respectively. Then, the obtained time-domain signals were processed by Fourier transform. The Faraday rotation angle can be derived using the following relation [34]:

$$\theta_F = \frac{1}{2}\arctan\frac{2\Re(E_x^* E_y)}{|E_x|^2 - |E_y|^2}. \quad (1)$$

Here, two mutually orthogonal complex electric field components (E_x and E_y) can be described using the complex electric field components of THz radiation transmitted through the system (Fig. 2) when the analyzer is set at 0° and 45° positions (complex E_0 and E_{+45}, respectively) as [35]:

$$\begin{pmatrix} E_x \\ E_y \end{pmatrix} = \begin{pmatrix} E_0 \\ -E_0 + 2E_{+45} \end{pmatrix}. \quad (2)$$

All of our spectroscopy experiments were performed at room temperature.

III. Results

The Faraday rotation spectra for several $BaAl_{1.4}Fe_{10.6}O_{19}$ samples with different thicknesses and densities are shown in Fig. 3.

As expected, the Faraday rotation angle increases for higher thicknesses of hexaferrite samples. Moreover, all the investigated samples exhibit broadband rotation. To implement a commonly used isolator based on the Faraday effect, the rotation angle of 45° should be achieved. The corresponding desired value of rotation angle is plotted by a dashed line in Fig. 3. The most relevant sample for usage as a THz isolator basis is the 2.8 mm-thick (№ 7) sample.

An important task is to predict the required thickness of the Faraday rotation medium for achieving 45° angle of polarization plane rotation. However, our previous study [31] revealed the strong dependence of the sample density on the Faraday rotation effect. Therefore, the dependence of θ_F on

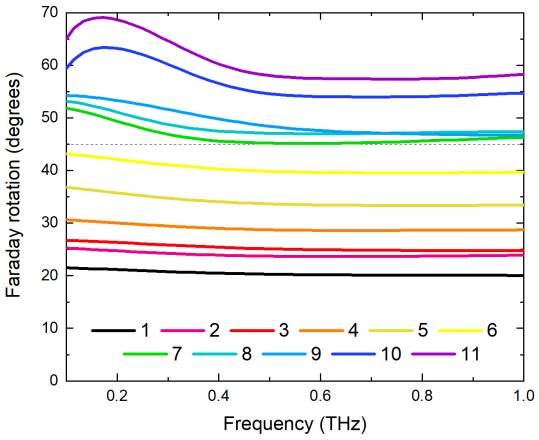

Fig. 3. Faraday rotation spectra of $BaAl_{1.4}Fe_{10.6}O_{19}$ with different thicknesses and densities. The notation for samples is set in accordance with Table I.

the surface density of the samples ($\rho \times d$) should be considered. Figure 4 shows the variation of the Faraday rotation angle against a product of hexaferrite thickness to its density ($\rho \times d$) at 0.4 THz.

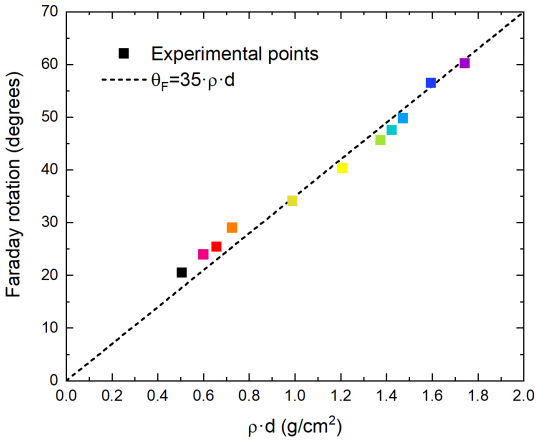

Fig. 4. Faraday rotation of $BaAl_{1.4}Fe_{10.6}O_{19}$ samples with different thicknesses and densities at 0.4 THz.

It is seen that the measured Faraday rotation is linearly proportional to the surface density of the samples. Corresponding approximation by linear function is also shown by a dashed line in Fig. 4. Using the obtained Faraday rotation experimental points at 0.4 THz we can define the coefficient relating the θ_F and the product $\rho \times d$, which is equal to 35 degrees$\times$cm^2/g.

Then, we have assembled the 2.8 mm-thick $BaAl_{1.4}Fe_{10.6}O_{19}$ sample into the Faraday isolator configuration (Fig. 5a). To do that, the hexaferrite was placed between two polarizers oriented at an angle of 45° relative to each other. The 1-inch polypropylene polarizers with 1200 lines per mm were used in isolator system [36]. The north pole of the hexaferrite was placed closer to the THz source. The transmission axis of the second polarizer (closer to the detector) was rotated by 45 degrees clockwise with respect to the transmission axis of the first polarizer. The isolation performance of the device was accessed by rotating the isolator system (hexaferrite and two polarizers) by 180° with respect to the direction of radiation propagation, using the following expression:

$$I_{so} = 10 \log \left(\frac{T_{for}}{T_{back}} \right), \tag{3}$$

where T_{for} is the forward transmission and T_{back} is the backward transmission through the isolator. The resulting isolation spectrum is shown in Fig. 5c.

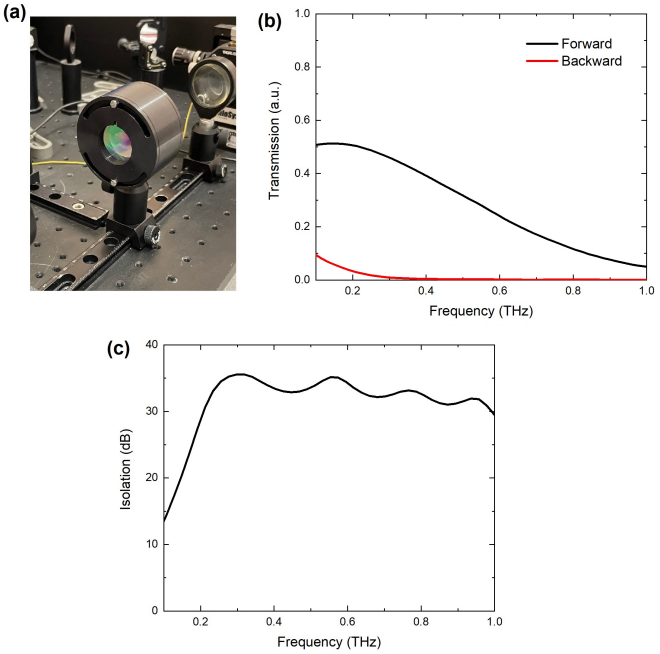

Fig. 5. Photograph of the isolator device based on 2.8 mm-thick $BaAl_{1.4}Fe_{10.6}O_{19}$ (a), its forward and backward transmission spectrum (b), and isolation spectrum (c).

The transmission in the forward direction decreases with the frequency increasing (Fig. 5b), defining the operational bandwidth. If we set the requirement on the minimum allowed transmission in the forward direction as 20%, the isolator operating range is up to 650 GHz. As seen from Fig. 5c the isolation spectrum exhibits broadband character with the maximum value of 35 dB at 0.3 THz. The lower isolation performance in the range from 0.1 THz to 0.2 THz is associated with the dispersion of Faraday rotation angle in this range (θ_F is higher than 45° at 0.1-0.2 THz). Rotation dispersion in this range is caused by the ferromagnetic resonance. Moreover, the isolation performance should be even higher for the reflected back wave (i.e., transmitted in the forward along with the backward direction). It is also known that hexaferrite samples have a high refractive index (more than 4) [31], which results in high reflection losses. In our case, the reflection losses can be expressed as $R = (\sqrt{\varepsilon} - 1)^2/(\sqrt{\varepsilon} + 1)^2 = 0.37$, where $\varepsilon = 16.8$ is the permittivity of the hexaferrite sample.

However, such losses can be reduced in a predefined frequency range by anti-reflection coatings.

To evaluate the performance of the designed THz isolator, the comparison with some best previously reported THz isolators is given in Table II. The advantage of the proposed isolator is in the broadest operation bandwidth at room temperature without applying external magnetic field.

IV. Discussion

In order to predict gyrotropy properties of hexaferrite samples without their direct measurements, we employ an approach based on permeability tensor derivation. The hexaferrite can be characterized by the permeability tensor as:

$$\bar{\bar{\mu}}(\omega) = \begin{pmatrix} \mu(\omega) & -j\kappa(\omega) & 0 \\ j\kappa(\omega) & \mu(\omega) & 0 \\ 0 & 0 & \mu_0 \end{pmatrix}, \tag{4}$$

where μ_0 is the vacuum permeability, while the tensor elements $\mu(\omega)$ and $\kappa(\omega)$ are expressed using the following relations:

$$\mu(\omega) = \mu_0 \left(1 - \frac{\omega_0 \omega_m}{\omega^2 - \omega_0^2}\right), \tag{5}$$

$$\kappa(\omega) = \mu_0 \frac{\omega \omega_m}{\omega^2 - \omega_0^2}. \tag{6}$$

In Eqs. 5, 6 ω_0 is the Larmor precession frequency, ω_m is the saturation magnetization frequency, which are expressed as:

$$\omega_0 = \mu_0 \gamma H_i, \tag{7}$$

$$\omega_m = \mu_0 \gamma M_s, \tag{8}$$

where H_i is the internal magnetic field, M_s is the saturation magnetization and $\gamma = -e/m_e = -1.7592 \times 10^{11}$ C/kg is the gyromagnetic ratio.

Faraday rotation angle is proportional to the ferrite thickness (d) and can be calculated as:

$$\theta_F = \frac{k_+ - k_-}{2} d, \tag{9}$$

where k_+ and k_- are the propagation constants for the right-hand circularly polarized (RHCP) and the left-hand circularly polarized (LHCP) waves, respectively. The propagation constants can be represented with effective permeability for the RHCP wave ($\mu + \kappa$) and the LHCP wave ($\mu - \kappa$) using the following expressions:

$$k_+ = \omega \sqrt{\varepsilon_0 \varepsilon (\mu + \kappa)}, \tag{10}$$

$$k_- = \omega \sqrt{\varepsilon_0 \varepsilon (\mu - \kappa)}, \tag{11}$$

where ε_0 is the vacuum permittivity, and $\varepsilon = 16.8$ is the extracted permittivity of the ferrite using transmission-mode terahertz time-domain spectroscopy method described in [38] for the investigated frequency range.

The saturation magnetization (M_s) can be determined as $4\pi M_s = 4\pi m_s / m\rho$ (m is the sample mass, ρ is the sample density) by measuring magnetic moment m_s using vibrating sample magnetometry. The saturation magnetization for 45°-rotating sample (№ 7) was found to be 205 kA/m.

The internal magnetic field in hexaferrite is defined as [27]:

$$H_i = H_A + H_{ext} + H_d, \tag{12}$$

where H_A is the anisotropic magnetocrystalline field, $H_{ext} = 0$ kA/m is the external applied field, and H_d is the demagnetizing field. The $BaAl_{1.4}Fe_{10.6}O_{19}$ sample has a strong anisotropy field $H_A = 1790$ kA/m, which was measured by the gyromagnetic resonance (GMR) method in a constant magnetic field. The demagnetization field is $H_d = -M$, where $M = 195$ kA/m is the magnetization of the ferrite obtained from magnetic hysteresis loop (see Fig. 6).

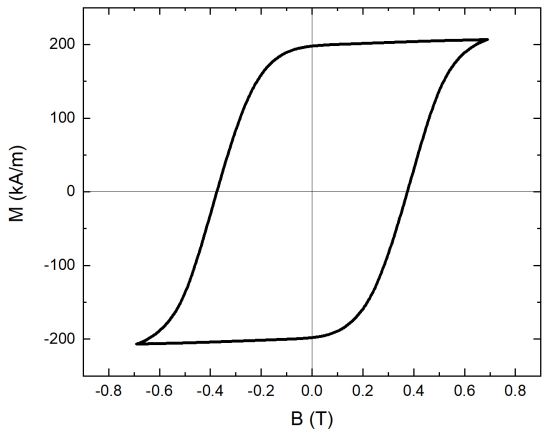

Fig. 6. Magnetic hysteresis loop of the 2.8 mm-thick $BaAl_{1.4}Fe_{10.6}O_{19}$ sample.

Fig. 7 demonstrates the Faraday rotation spectrum obtained using Eqs. 5-12.

The close agreement between the predicted and measured values of the Faraday rotation in Fig. 7 confirms the reliability of the utilized approach. Thus, the gyrotropy properties of hexaferrite ceramics in the THz frequency range can be estimated by their magnetic properties. The difference between calculated and measured data in the low-frequency region is associated with the neglection of the losses in calculation for simplicity. In reality, the losses lead to the damping out of the ferromagnetic resonance.

V. Conclusion

To conclude, we presented a complete broadband THz isolator that operates without external magnetic bias at room temperature. The high-dense $BaAl_{1.4}Fe_{10.6}O_{19}$ magneto-optical hexaferrite was chosen as a basis of the nonreciprocal isolator with Faraday geometry. We have obtained over 30 dB of isolation in the 0.2-1 THz band. We found a relation between Faraday rotation and surface density of the hexaferrite

TABLE II
COMPARISON OF DERIVED RESULTS WITH RECENTLY REPORTED STUDIES ON THZ ISOLATORS.

Reference	Maximum isolation	Operating temperature	External magnetic field	Bandwidth
[26]	-	room	0 T	up to 500 GHz
[24]	20 dB	room	7 T	50 GHz
[20]	35 dB	room	0.2-0.35 T	45 GHz
[23]	18.8 dB	180 K	0.13 T	0.8–1.3 THz
[37]	52 dB	room	0.68 T	0.14 GHz
[this work]	35 dB	room	0 T	up to 650 GHz

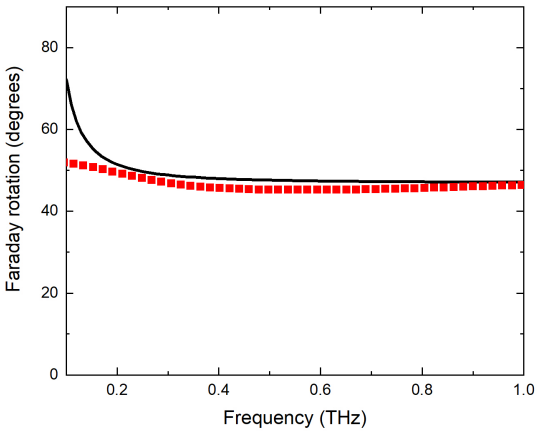

Fig. 7. Faraday rotation spectra for 2.8 mm-thick $BaAl_{1.4}Fe_{10.6}O_{19}$ sample: measured value (red symbols) and calculated data using Eq. 9 (black solid line).

ceramics. At the same time, we have verified an approach for the prediction of hexaferrite gyrotropy characteristics only through its magnetic properties. Finally, we emphasize that the proposed devise accommodates high isolation performance with a simple design.

ACKNOWLEDGMENT

This work was performed using the resources of Tydex LLC. The authors would like to thank the Interdisciplinary Resource Center for collective usage "Modern physicochemical methods for the formation and research of materials for the needs of industry, science and education" of the Herzen State Pedagogical University of Russia for the XRD measurements.

REFERENCES

[1] D. M. Mittleman, "Perspective: Terahertz science and technology," *Journal of Applied Physics*, vol. 122, no. 23, p. 230901, 2017.
[2] S. Dhillon, M. Vitiello, E. Linfield, A. Davies, M. C. Hoffmann, J. Booske, C. Paoloni, M. Gensch, P. Weightman, G. Williams *et al.*, "The 2017 terahertz science and technology roadmap," *Journal of Physics D: Applied Physics*, vol. 50, no. 4, p. 043001, 2017.
[3] X. C. Zhang, A. Shkurinov, and Y. Zhang, "Extreme terahertz science," *Nature Photonics*, vol. 11, no. 1, pp. 16–18, 2017.
[4] S. L. Dexheimer, *Terahertz spectroscopy: principles and applications*. CRC press, 2017.
[5] M. Naftaly, N. Vieweg, and A. Deninger, "Industrial applications of terahertz sensing: state of play," *Sensors*, vol. 19, no. 19, p. 4203, 2019.
[6] D. M. Mittleman, "Twenty years of terahertz imaging," *Optics express*, vol. 26, no. 8, pp. 9417–9431, 2018.
[7] T. Nagatsuma, G. Ducournau, and C. C. Renaud, "Advances in terahertz communications accelerated by photonics," *Nature Photonics*, vol. 10, no. 6, pp. 371–379, 2016.
[8] V. S. Asadchy, M. S. Mirmoosa, A. Díaz-Rubio, S. Fan, and S. A. Tretyakov, "Tutorial on electromagnetic nonreciprocity and its origins," *Proceedings of the IEEE*, vol. 108, no. 10, pp. 1684–1727, 2020.
[9] C. Caloz, A. Alu, S. Tretyakov, D. Sounas, K. Achouri, and Z.-L. Deck-Léger, "Electromagnetic nonreciprocity," *Physical Review Applied*, vol. 10, no. 4, p. 047001, 2018.
[10] F. Fan, S. Chen, and S.-J. Chang, "A review of magneto-optical microstructure devices at terahertz frequencies," *IEEE Journal of Selected Topics in Quantum Electronics*, vol. 23, no. 4, pp. 1–11, 2016.
[11] X. Wang, A. Diaz-Rubio, H. Li, S. A. Tretyakov, and A. Alu, "Theory and design of multifunctional space-time metasurfaces," *Physical Review Applied*, vol. 13, no. 4, p. 044040, 2020.
[12] A. Shaltout, A. Kildishev, and V. Shalaev, "Time-varying metasurfaces and lorentz non-reciprocity," *Optical Materials Express*, vol. 5, no. 11, pp. 2459–2467, 2015.
[13] D. L. Sounas, J. Soric, and A. Alu, "Broadband passive isolators based on coupled nonlinear resonances," *Nature Electronics*, vol. 1, no. 2, pp. 113–119, 2018.
[14] Y. Shi, Z. Yu, and S. Fan, "Limitations of nonlinear optical isolators due to dynamic reciprocity," *Nature photonics*, vol. 9, no. 6, pp. 388–392, 2015.
[15] T.-F. Li, Y.-L. Li, Z.-Y. Zhang, Q.-H. Yang, F. Fan, Q.-Y. Wen, and S.-J. Chang, "Terahertz faraday rotation of magneto-optical films enhanced by helical metasurface," *Applied Physics Letters*, vol. 116, no. 25, p. 251102, 2020.
[16] I. Crassee, J. Levallois, A. L. Walter, M. Ostler, A. Bostwick, E. Rotenberg, T. Seyller, D. Van Der Marel, and A. B. Kuzmenko, "Giant faraday rotation in single-and multilayer graphene," *Nature Physics*, vol. 7, no. 1, pp. 48–51, 2011.
[17] T. Arikawa, X. Wang, A. A. Belyanin, and J. Kono, "Giant tunable faraday effect in a semiconductor magneto-plasma for broadband terahertz polarization optics," *Optics express*, vol. 20, no. 17, pp. 19 484–19 492, 2012.
[18] A. Shuvaev, G. Astakhov, A. Pimenov, C. Brüne, H. Buhmann, and L. Molenkamp, "Giant magneto-optical faraday effect in hgte thin films in the terahertz spectral range," *Physical review letters*, vol. 106, no. 10, p. 107404, 2011.
[19] F. Fan, S.-J. Chang, W.-H. Gu, X.-H. Wang, and A.-Q. Chen, "Magnetically tunable terahertz isolator based on structured semiconductor magneto plasmonics," *IEEE Photonics Technology Letters*, vol. 24, no. 22, pp. 2080–2083, 2012.
[20] S. Lin, S. Silva, J. Zhou, and D. Talbayev, "A one-way mirror: High-performance terahertz optical isolator based on magnetoplasmonics," *Advanced Optical Materials*, vol. 6, no. 19, p. 1800572, 2018.
[21] Y. Ji, F. Fan, Z. Tan, and S. Chang, "Terahertz nonreciprocal isolator based on magneto-plasmon and destructive interference at room temperature," *Frontiers in Physics*, vol. 8, p. 334, 2020.
[22] S. Chen, F. Fan, X. Wang, P. Wu, H. Zhang, and S. Chang, "Terahertz isolator based on nonreciprocal magneto-metasurface," *Optics express*, vol. 23, no. 2, pp. 1015–1024, 2015.
[23] E. Keshock, P. Peng, J. Zhou, and D. Talbayev, "Nonreciprocal fabry-perot effect and performance enhancement in a magneto-optical insb-based faraday terahertz isolator," *Optics Express*, vol. 28, no. 25, pp. 38 280–38 292, 2020.
[24] M. Tamagnone, C. Moldovan, J.-M. Poumirol, A. B. Kuzmenko, A. M. Ionescu, J. R. Mosig, and J. Perruisseau-Carrier, "Near optimal graphene terahertz non-reciprocal isolator," *Nature communications*, vol. 7, no. 1, pp. 1–6, 2016.
[25] D. H. Martin and R. J. Wylde, "Wideband circulators for use at frequencies above 100 ghz to beyond 350 ghz," *IEEE Transactions on Microwave Theory and Techniques*, vol. 57, no. 1, pp. 99–108, 2008.

[26] M. Shalaby, M. Peccianti, Y. Ozturk, and R. Morandotti, "A magnetic non-reciprocal isolator for broadband terahertz operation," *Nature communications*, vol. 4, no. 1, pp. 1–7, 2013.
[27] T. Horák, G. Ducournau, M. Mičica, K. Postava, J. B. Youssef, J.-F. Lampin, and M. Vanwolleghem, "Free-space characterization of magneto-optical hexaferrites in the submillimeter-wave range," *IEEE Transactions on Terahertz Science and Technology*, vol. 7, no. 5, pp. 563–571, 2017.
[28] B. Yang, R. J. Wylde, D. H. Martin, P. Goy, R. S. Donnan, and S. Caroopen, "Determination of the gyrotropic characteristics of hexaferrite ceramics from 75 to 600 ghz," *IEEE transactions on microwave theory and techniques*, vol. 58, no. 12, pp. 3587–3597, 2010.
[29] B. Yang, X. Wang, Y. Zhang, and R. S. Donnan, "Experimental characterization of hexaferrite ceramics from 100 ghz to 1 thz using vector network analysis and terahertz-time domain spectroscopy," *Journal of Applied Physics*, vol. 109, no. 3, p. 033509, 2011.
[30] C. Yu, Y. Zeng, B. Yang, R. Wylde, R. Donnan, J. Wu, J. Xu, F. Gao, I. Abrahams, M. Reece *et al.*, "Srfe12o19 based ceramics with ultra-low dielectric loss in the millimetre-wave band," *Applied Physics Letters*, vol. 112, no. 14, p. 143501, 2018.
[31] A. Grebenchukov, V. Ivanova, G. Kropotov, and M. Khodzitsky, "Terahertz faraday rotation of aluminum-substituted barium hexaferrite," *Applied Physics Letters*, vol. 118, no. 19, p. 191104, 2021.
[32] J. Rodríguez-Carvajal, "Recent advances in magnetic structure determination by neutron powder diffraction," *Physica B: Condensed Matter*, vol. 192, no. 1-2, pp. 55–69, 1993.
[33] A. Trukhanov, V. Turchenko, I. Bobrikov, S. Trukhanov, I. Kazakevich, and A. Balagurov, "Crystal structure and magnetic properties of the bafe12- xalxo19 (x= 0.1–1.2) solid solutions," *Journal of Magnetism and Magnetic Materials*, vol. 393, pp. 253–259, 2015.
[34] M. Born and E. Wolf, *Principles of optics: electromagnetic theory of propagation, interference and diffraction of light*. Elsevier, 2013.
[35] K.-E. Peiponen, A. Zeitler, and M. Kuwata-Gonokami, *Terahertz spectroscopy and imaging*. Springer, 2012, vol. 171.
[36] "Optical components and instruments for research and industry." [Online]. Available: http://www.tydexoptics.com/
[37] S. Yuan, L. Chen, Z. Wang, W. Deng, Z. Hou, C. Zhang, Y. Yu, X. Wu, and X. Zhang, "On-chip terahertz isolator with ultrahigh isolation ratios," *Nature Communications*, vol. 12, no. 1, pp. 1–8, 2021.
[38] M. Naftaly, *Terahertz metrology*. Artech House, 2015.

Alexander N. Grebenchukov graduated as an Engineer with honors in electronic devices from TUSUR University, Tomsk, Russia, in 2013. He received the Ph.D. degree in optics from ITMO University, St. Petersburg, Russia, in 2020. He is currently a Research Associate at Tydex LLC. His current research interests include terahertz metamaterials and nonreciprocal terahertz devices.

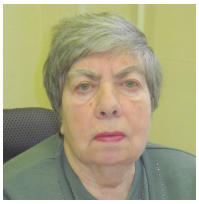

Valentina I. Ivanova was born in Leningrad, USSR, in 1938. She graduated as an Engineer in semiconductors and dielectrics from Polytechnic University, Leningrad, in 1962. She received a Ph.D. degree in semiconductor technology and materials for electronics. In 2006, she was awarded the title of Senior Research Scientist. She is currently a leading specialist with the Ferrite-Domen Scientific Research Institute, St.Petersburg. Her current research interests include polycrystalline hexaferrites and ceramic materials for microwave devices. She has authored or coauthored over 50 papers and more than 30 patents.

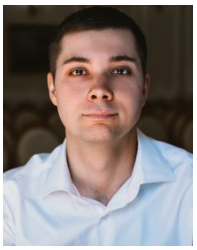

Anton V. Suslov was born in Russia in 1990. He received the M.S. degree in physics and a Ph.D. degree in condensed matters physics from the Herzen State Pedagogical University of Russia in 2016 and 2020, respectively. He is currently an engineer with the Herzen State Pedagogical University of Russia. His research interests include XRD analysis, physics of thin films, and nanostructure of semimetals and semiconductors.

Grigory I. Kropotov holds M.S. with honors in Engineering Physics with specialization in Optical and Electronic Devices from the State Technical University (1977, Leningrad, USSR), and Ph.D. in Physics and Mathematics from the same University (1983). He had twenty-year experience (from 1974 till 1994) at the Ioffe Physical-Technical Institute of Russian Academy of Sciences in basic researches in various fields of physics: semiconductors (Ge, Si, narrow-gap and semi-magnetic compounds), FIR molecular lasers, FTIR spectroscopy, strong magnetics, and cryogenics. Grigory has a diploma of Senior Research Scientist of the Russian Academy of Sciences (1993, St.Petersburg, Russia). Grigory became the Commercial Director of the private company Tydex, LLC after its foundation in 1994 and later since 2002 General Manager (CEO). Grigory has been the only owner of the company since 2011. He has 5 Best Research Awards (1981, 1982, 1984, 1985, 1988) from the Ioffe Institute and the Russian Academy of Sciences and the Personal Grant from the International Science Foundation (1993). Since 2008 Grigory's scientific interests include different aspects of R&D and the production of terahertz instruments, accessories, and components. Grigory is an author of several patents and over 50 publications.

Mikhail K. Khodzitsky was born in Sumy, USSR in 1984. He received MSc with honors in Laser and Optoelectronic techniques from the Kharkov National University of Radioelectronics (2005, Kharkov), Ph.D. in Radiophysics from Institute of Radiophysics and Electronics of NASU (2010, Kharkov), Ph.D. in Optics and Radiophysics from ITMO University (2013, Saint Petersburg, Russia). He had twenty-year of experience in millimeter, microwave, terahertz, and optical devices and applications. He has several awards: Sinelnikov's scholarship on physics for young scientists (2008); SPIE Educational Scholarship (2009, 2010, 2011, 2012); IEEE MTTs Graduate Fellowship Award (2010); Grant for young scientists of "Dynasty" Foundation (2011); the best young scientist of ITMO University (2014, 2016); Award of the Government of St. Petersburg in the field of scientific and pedagogical activity (2016, 2017). SPIE Fellowship award (2020). He is an author of several patents and over 180 publications. He is chief of THz biomedicine Laboratory since 2013 (ITMO University) and head of the Research and Development Department since 2020 (Tydex, LLC).